

Weakly mass-loaded accretion disks

Yuri A. Shchekinov*

Department of Physics, University of Rostov,
Rostov on Don, 344090 Russia

December 2, 2024

Abstract

Accretion disks with an additional mass input on the disk surface from environment are considered in the limit of low mass input rate, *i.e.* when the accretion flow remains keplerian. Due to dissipation of kinetic energy of the infalling gas disk temperature increases, and can deviate significantly from standard temperature of reprocessing accretion disks in their outer regions. This increase in temperature produces an excess of emission in a long-wavelength range of the disk spectrum. An illustrative example of the spectrum of a weakly mass-loaded disk (the surface mass input rate $\dot{M}_{\text{load}} \simeq 1.5 \times 10^{-8} M_{\odot} \text{ yr}^{-1}$) reasonably reproducing FIR excess observed in CS Chameleon is given.

*yus@phys.rnd.runnet.ru

1 Introduction

Dynamics of the multi-phase interstellar medium is dominated by mass and momentum exchange between different phases. Ejection of mass into diffuse component from a condensed phase changes velocity of the bulk flow, increases pressure in diffuse phase, and heats diffuse gas due to conversion of kinetic energy of evaporated/destroyed clouds into thermal energy of bulk medium (Cowie, McKee & Ostriker 1981, Hartquist *et al.* 1986). As a result, loaded flows (*i.e.* the flows dominated by mass input from a condensed phase) can differ qualitatively from the ones in a homogeneous (monophase) medium. In a simplest approach mass loaded flows are described by dynamical equations with source terms. For accretion disks mass loading corresponds physically to a continuing mass infall on the disk surface from the residual gas envelope.

Extremely inhomogeneous structure of the diffuse interstellar gas and molecular clouds shows self-similarity on the scales from 0.02 (the resolution threshold) to 100 pc (see, Falgarone, Phillips & Walker 1991). It seems obvious that such self-similarity can extend to much smaller scales corresponding to protoplanetary condensations in accretion disks. [Note that the resolution limit, 0.02 pc, corresponds to planetary masses of clumps, $\sim 10^{-4} M_{\odot}$]. One can expect that in such conditions clumpy gas from debris of the parent molecular cloud will provide a continuing matter infall on the accretion protoplanetary disk being already formed. In theoretical treatment of protoplanetary disks this circumstance is described by the source terms in mass and momentum equations (see, *e.g.* Safronov & Vityazev 1983, Papaloizou & Lin 1995). Multiple CI and CO velocity components (Roberge *et al.* 2000), CaII absorptions (Barnes, Tobin & Pollard 2000) and emission in FeII, SiI, SiII, NiII and CI lines (Lecavelier des Etangs *et al.* 2000), observed in β Pictoris, are seemingly connected with the infall of clumpy gas on the disk. Similar detections of the infalling circumstellar gas have been reported for Herbig Ae/Be stars (Grinin, Natta & Tambovtseva 1996). One can assume that this phenomenon represents late stages of matter infall from a highly inhomogeneous primordial circumdisk cloud onto the accretion disk. If this is the case, and protoplanetary disks are loaded by infalling and passing through them dense clumps, both vertical and radial structure of such disks, the accretion rate and the temperature distribution can differ considerably from those in homogeneous (monophase) disks. In this paper we analyze

properties of steady disks, concentrating mainly on radial temperature distribution, in a simple model of weak mass loading, *i.e.* when mass loading does not violate the keplerian flow of the bulk motion. In Section 2.1 we describe the model, in Section 2.2 we formulate basic equations describing radial structure of thin accretion disks for weak mass loading limit, in Section 2.3 we describe the solution of energy equation and find radial temperature distribution, and discuss possible observational manifestations, the effects of angular momentum input associated with mass loading on temperature distribution are discussed in Sec. 2.4, Section 3 summarizes the results.

2 Model and governing equations

2.1 Model of weakly loaded disks

As a model of a mass-loaded disk which admits simple analytical description we will accept the following: an accretion disk is surrounded by a spherical “subsystem” of dense condensations formed of the debris of a parent cloud and orbiting around the central star (Fig. 1). This subsystem can be in a quasistationary state either because the condensations are nearly dissipationless, or an infinite (in practice, very massive) reservoir of gas replenishes dissipation of mass and energy. In the first case, the characteristic life time of the quasistationary orbits determined by interaction of the condensations with the diffuse component, with other condensations and with the disk itself, must be much larger than characteristic rotation period of the disk. For this to fulfill the following relations must hold, respectively

$$N_i \ll N_c, \quad \langle N_c \rangle \ll N_c, \quad N_d \ll N_c, \quad (1)$$

where N_i , N_c , and N_d are the column densities of the diffuse intercloud gas over the whole circumdisk cloud, of a single clump, and of the disk, respectively, $\langle N_c \rangle = fN_c$, $f = \mathcal{N}_c R_c^2 / R^2$ is the covering factor of clumps, R_c is the clump radius, R , the radius of the circumdisk cloud. These inequalities definitely fulfill for planetesimals or comet-like bodies. For gaseous clumps it is not so obvious, and one has to assume a large enough density contrast in order that the clumps were long-living and orbiting quasistationary. In the latter case when the clumps are not sufficiently dense, so that for instance

$N_c \sim N_d$ and they are absorbed by the disk in a single encounter, the overall picture can be kept quasistationary due to replenishment of the clumps from the surrounding molecular cloud as shown schematically on Fig. 1. A gas reservoir with radius $R \sim 3 - 10$ pc can support continuous mass infall during the time $t \sim 1 - 3$ Myr with the rate $10^{-7} - 10^{-6} M_\odot \text{ yr}^{-1}$ if the mean density is only $n_c f_v \sim 0.03 - 0.3 \text{ cm}^{-3}$, where n_c is gas density in clumps, f_v , the volume filling factor of the clumps; optical depth corresponding to the whole ensemble of such clumps is as small as $\tau_c \sim 10^{-21} n_c f_v R \sim 0.03$. As we will see below, mass loading even with one order of magnitude lower mass rate can produce observable effects. We will assume that the quasistationarity takes place in either way. With these assumptions the subsystem of clumps can be treated as stationary. When the clumps intersect the disk they lose a fraction of their mass due to stripping under the action of Rayleigh-Taylor instability (see detailed discussion in Hartquist *et al.* 1986, Klein, McKee & Colella 1994). The subsystem of clumps is assumed in rest as a whole, *i.e.* $\langle \mathbf{v}_c(\mathbf{r}) \rangle = 0$, where the averaging is over the ensemble of clumps at given \mathbf{r} , such that the angular momentum input into the disk from destroying clumps is zero. More general case with $\mathbf{v}_c = \mathbf{v}_c(\mathbf{r})$ will be discussed in Sec. 2.4.

2.2 Equations of motions

In this framework the continuity equation for thin disk is described by the equation

$$\frac{1}{R} \frac{d}{dR} (R \Sigma u_R) = \Psi, \quad (2)$$

where $\Sigma = \int_{-\infty}^{+\infty} \rho dz$, $u_R = \int_{-\infty}^{+\infty} v_r dz$, (the interrelation $\Sigma u_R = \int_{-\infty}^{+\infty} \rho v_r dz$ is assumed as well), $\Psi = \int_{-\infty}^{+\infty} q dz$, q [$\text{g cm}^{-3} \text{ s}^{-1}$] is the mass ejection rate from destroying clumps per unit volume. [In general, Ψ may represent not only mass loading due to destroying cloudlets, but also mass infall onto the disk from the envelope (Safronov & Vityazev 1983), the effects of the mass transfer stream in cataclismic variable stars, and the mass loss through a wind (Papaloizou & Lin 1995)].

Navier-Stokes equation for azimuthal component of a stationary disk with zero angular momentum input is written in a standard form (see, Shakura & Sunyaev 1973, Pringle 1981)

$$\frac{d}{dR}(\Sigma R^3 \Omega u_R) = \frac{d}{dR} \left(\nu \Sigma R^3 \frac{d}{dR} \Omega \right), \quad (3)$$

here $u_\phi = \Omega R$ is explicitly taken into account, $\Omega = \Omega(R)$ is the local angular velocity, ν is the kinematical viscosity. The change of the angular velocity Ω in one rotational period $T_R = 2\pi/\Omega$ due to mass input is $|\Delta\Omega| \sim \Psi/\Sigma$. From requirement that $|\Delta\Omega|/\Omega \ll 1$ one obtains restriction on the mass loading $\Psi \ll \Sigma\Omega/2\pi$, so that the ratio of the mass input rate \dot{M}_p associated with the infalling clumps to the standard mass accretion rate $\dot{M}_0 \sim 2\pi\nu\Sigma$ is

$$\frac{\dot{M}_p}{\dot{M}_0} \ll \frac{1}{4\pi} \frac{R^2 \Omega}{\nu} \sim \frac{1}{4\pi} \frac{u_\phi}{|u_R|} \gg 1. \quad (4)$$

Obviously, the restrictions on the mass input Ψ are rather weak. Formally, the change in Ω is larger on a much longer accretion time, $T_D = R/|u_R| \sim R^2/\nu$ (here $u_R \sim \nu/R$ is explicitly assumed, see Pringle 1981)

$$|\Delta\Omega| \sim \Omega_0 \frac{\dot{M}_p}{\dot{M}_0}, \quad (5)$$

where Ω_0 is characteristic angular velocity in the absence of mass loading.

For the radial velocity component we have

$$u_R \frac{du_R}{dR} - \frac{u_\phi^2}{R} + \frac{1}{\rho} \frac{dp}{dR} + \frac{GM}{R^2} = -\frac{\Psi u_R}{\Sigma}. \quad (6)$$

Assuming that for a weak loading the radial component u_R is of the order ν/R (see, Pringle 1981) we arrive at

$$u_\phi^2 = \frac{GM}{R} \left[1 + O(\mathcal{M}^{-2}) + \beta(R) \right], \quad (7)$$

where $\beta = \Psi u_R R^2 / GM \Sigma$, $\mathcal{M} = u_\phi / c_s$ is the local azimuthal Mach number, c_s , the local sound speed. Equations 2-6 differ from the standard equations of thin accretion disk (Shakura & Sunyaev 1973, Lyndel-Bell & Pringle 1974, see also reviews by Pringle 1981, and Papaloizou & Lin 1995) by the sources due to mass loading in the r.h.s. of continuity equation 2 and in equation for radial velocity, eq. 6. The parameter β can be estimated as

$$\beta \sim \frac{\alpha T_R}{\pi T_D} \frac{\dot{M}_p}{\dot{M}_0} \ll 1, \quad (8)$$

with the assumption that \dot{M}_p/\dot{M}_0 can have low or moderately high values, here α is the viscosity parameter (Shakura & Sunyaev 1973), and thus its contribution to the r.h.s. of eq. 7 is negligible, and in this sense the loading will be treated as weak. It is readily seen that approximately $\beta \sim 2\pi\Psi/\Omega\Sigma$, and eq. 8 is equivalent to the condition that on one rotational period $|\Delta\Omega| \ll \Omega$. This means that the infalling settles onto the generic keplerian motion quickly, and as long as the mass input from clumpuscles is small enough on one rotational period, *i.e.* eq. 4 fulfills, it can be treated as a weak loading.

Defining the accretion rate as $\dot{M} = -2\pi R\Sigma u_R$ (see Pringle 1981) one can obtain the following solutions of equations 2 and 3 for a weakly loaded (*i.e.* $\beta \ll 1$) disk

$$\dot{M} = \dot{M}_* - 2\pi \int_{R_*}^R \Psi R dR, \quad (9)$$

$$\nu\Sigma = \frac{\dot{M}_*}{3\pi} \left[1 - \left(\frac{R_*}{R} \right)^{1/2} \right] - \frac{2}{3} \int_{R_*}^R \Psi R dR, \quad (10)$$

where $\dot{M}_* = -2\pi(R\Sigma u_R)_*$ is the total mass accretion rate (*i.e.* the rate on the stellar surface); note, that the mass rate provided by the accretion disk itself in the absence of mass loading is equal

$$\dot{M}_0 = \dot{M}_* - 2\pi \int_{R_*}^{\infty} \Psi R dR. \quad (11)$$

The quantity $\nu\Sigma$ determines dissipation at a rate

$$D(R) = \frac{1}{2}\nu\Sigma(R\Omega')^2 = \frac{3GM\dot{M}_*}{8\pi R^3} [1 - (R_*/R)^{1/2}] - \frac{3GM}{4R^3} \int_{R_*}^R \Psi(R) R dR, \quad (12)$$

and the corresponding luminosity integrated over the disk

$$L_D^\nu = 4\pi \int_{R_*}^{\infty} D(R) R dR = \frac{1}{2} \frac{GM\dot{M}_*}{R_*} - 3\pi GM \int_{R_*}^{\infty} \frac{dR}{R^2} \int_{R_*}^R \Psi(R') R' dR'. \quad (13)$$

2.3 Energy equation

One of the most interesting and important consequence of the mass loading is connected with possible heating of the disk due to conversion of kinetic energy of the falling gas into heat. The energy equation in the presence of mass loading (see, Cowie, McKee & Ostriker 1981, White & Long 1991), integrated over z , is written as

$$\Sigma \dot{\varepsilon} = \frac{3}{2} \frac{\mathcal{R}}{\mu} T \Psi \left[\frac{1}{2} (\gamma - 1) \frac{\rho \langle u^2 \rangle}{p} - \gamma \right] + \frac{1}{2} \nu \Sigma (R \Omega')^2 - \mathcal{L}(T, \rho), \quad (14)$$

where ε is specific (per unit mass) thermal energy, the first term in the r.h.s. describes the energy input due to inelastic interaction of gas stripped from clumps and involved in keplerian motion of the disk, $\langle u^2 \rangle$ is the mean square relative velocity of clumps and disk (the averaging is over the ensemble of clumps), \mathcal{R} is gas constant, \mathcal{L} is the radiative cooling rate, we will assume $\mathcal{L} = \sigma T^4$, σ is Stefan-Boltzmann constant, the second term is the dissipative energy rate, eq. 12. In steady case, disk temperature is determined

$$\sigma T^4 = \frac{3}{2} \frac{\mathcal{R}}{\mu} T \Psi \left[\frac{1}{2} (\gamma - 1) \frac{\rho \langle u^2 \rangle}{p} - \gamma \right] + \frac{1}{2} \nu \Sigma (R \Omega')^2. \quad (15)$$

The mean square velocity is $\langle u^2 \rangle = u_\phi^2 + u_c^2$, where u_c is the velocity dispersion of clumps encountering the disk, for clumps orbiting around the central star or falling from external molecular cloud $u_c \sim u_\phi$, so we will assume $\langle u^2 \rangle \simeq 2u_\phi^2$; the contribution from radial disk velocity u_R is neglected. The corresponding contribution to disk luminosity from the first term in the r.h.s. of eq. 14 is

$$L_D^c = 6\pi \frac{\mathcal{R}}{\mu} \int_{R_*}^{\infty} T \Psi \left[\frac{1}{2} (\gamma - 1) \frac{\rho \langle u^2 \rangle}{p} - \gamma \right] R dR, \quad (16)$$

and when compared to the viscous luminosity in the absence of mass loading it is

$$\frac{L_D^c}{L_{D0}^c} \sim \frac{R^2 \Psi}{\nu \Sigma} \sim \frac{\dot{M}_p}{\dot{M}_0}. \quad (17)$$

In dimensionless units eq. 15 reads as

$$\theta^4 + 6\delta \frac{\Lambda - 1}{I} \psi \theta = 2(\gamma - 1) \frac{\Lambda - 1}{I} \frac{\psi}{x} + \frac{\Lambda}{x^3} \left(1 - \frac{1}{\sqrt{x}}\right) - \frac{\Lambda - 1}{I} \frac{1}{x^3} \int_1^x \psi x dx, \quad (18)$$

where $x = R/R_*$, Ψ assumed in the form $\Psi = \Psi_0 \psi(x)$, $\theta = T/T_*$, $\delta = (c_*/c_M)^2$

$$T_* = \left(\frac{3GM\dot{M}_0}{8\pi\sigma R_*^3} \right)^{1/4}, \quad \Lambda = \frac{\dot{M}_*}{\dot{M}_0}, \quad \dot{M}_* = 2\pi\Psi_0 R_*^2 I + \dot{M}_0, \\ I = \int_1^\infty \psi x dx, \quad c_*^2 = \gamma \frac{\mathcal{R}}{\mu} T_*, \quad c_M^2 = \frac{GM}{R_*}. \quad (19)$$

The problem contains two dimensionless parameters, δ , and Λ . It is readily seen that $\delta \ll 1$: for $R_* = R_\odot$, $M = M_\odot$ and $\dot{M}_0 \sim 10^{-6} M_\odot \text{ yr}^{-1}$ this ratio is $\delta \simeq 10^{-3}$. For weak loading, *i.e.* $\dot{M}_* \gtrsim \dot{M}_0$, $\Lambda - 1$ is also small, however even in this case mass loading can change significantly temperature distribution in the disk and its spectrum. In Fig. 2 we show the temperature distribution $\theta(x)$ for the mass-loading function

$$\psi(R) = \left[\frac{R - R_*}{R_L} \right] \exp\left(-\frac{R - R_*}{R_L} + 1\right), \quad (20)$$

with the peak $\psi(R) = 1$ at $R = R_* + R_L$, where R_L is the scale of the radial distribution of matter infall, $R_L = LR_*$, $L = 30$ and a set of Λ .

It is seen that the most important contribution from additional mass input comes from regions $x \gtrsim L$ where temperature can increase by factor of 2 even for a moderate mass loading $\Lambda = 2$. At larger distances, $x \sim 10 - 20 L$, the temperature profiles for $\Lambda > 1$ approach the standard profile ($\Lambda = 1$), and then go lower because at such distances the heat input from kinetic energy of clumps ($u^2 \propto x^{-1}$, first term in the r.h.s. of eq. 18) is smaller than the energy required to heat the infalling (presumably cold) gas (second term in the l.h.s. of eq. 18). Similar changes are seen for more extended in radius mass input, $L = 100$ (Fig. 3). In this case, the surface mass input rate for equal Λ is ~ 3 times lower than for $L = 30$, as $\Lambda - 1 \propto \Psi_0 L$, however the increase in total luminosity of loaded disks from the area $\propto L^2$ must be larger. For mass input in the form eq. 20 and $\Lambda - 1 \sim 1$ at $x < L/3$ the

second term in the r.h.s. of eq. 18 dominates and the first and third terms contribute only around 0.01 % to 1%, at $x \gtrsim L/3$ the situation changes and main contribution (up to 97%) is from the first term in eq. 18. At $x > 10L$ the dominant contribution is again from the second term; the third term at $x > L/3$ remains always about 30-50 % of the second. For $\Lambda - 1 \sim 0.1$ the second term dominates up to $x \sim 2L/3$ and then at $x > 8L$, the last term always remains as small as 5-10 % of the second term.

In order to illustrate how the mass loading can change the spectra of accretion disks, we show here the spectral energy distribution (SED) for optically thick disks seen face-on

$$\Sigma_\nu = 2\pi \int_{R_*}^{R_{out}} B_\nu[T(R)] R dR, \quad (21)$$

with $T(R) = T_*\theta(x)$, $B_\nu[T]$ being the Planck function, R_{out} , the outer radius of the disk, in the models shown in Figs (2)–(5) $R_{out} = 500$, contribution from regions $R > 500$ is small. Defining dimensionless frequency y as

$$y = \frac{h\nu}{k_B T_*}, \quad (22)$$

one can reduce eq. 21 to the form

$$\Sigma_\nu = \Sigma_0 S(y), \quad (23)$$

where

$$\Sigma_0 = \frac{16\pi^2 k_B^3 T_*^3 R_*^2}{h^2 c^2}. \quad (24)$$

Fig. 4 shows the spectra from disks with temperature distribution shown in Fig. 2. It is seen that even for relatively small loading, $\Lambda = 2$, the spectrum changes substantially: in maximum it increases by factor of 5, the maximum itself is more sharp showing an excess of energy in this range (for $R = R_\odot$, $M = M_\odot$ and $\dot{M}_0 = 10^{-6} M_\odot \text{ yr}^{-1}$ the frequency at maximum is $\nu \sim 1 - 1.5 \times 10^{13}$ Hz, or $\lambda \sim 10 - 20 \mu\text{m}$). For a more extended disk ($L = 100$) the changes in their spectra are more pronounced as shown in Fig. 5: at $\Lambda = 2$ in maximum it reaches an order of magnitude increase in comparison with mass-unloaded disks, the maximum itself shifts to a lower frequencies, and the

energy excess in this frequency range is more obvious. These two examples show that additional heat input due to mass loading can be responsible (or may contribute) for FIR excess observed from circumstellar disks around young stars (see for a review Natta, Meyer, Beckwith 1997). In order to illustrate such a possibility we compare in Fig. 6 the spectrum expected from an optically thick mass-loaded disk seen face-on with the one observed in the Chameleon cloud (Natta *et al.* 1997). For the modelled spectrum we assumed the distribution of infalling material of $L = 9.2$ AU in radius (integration was over $R = 3L$), its accretion mass rate $\dot{M}_0 = 2.2 \times 10^{-7} M_\odot \text{ yr}^{-1}$, and the mass loading only $\Lambda - 1 = 0.08$, the central star is of $M = 1 M_\odot$, $R_* = R_\odot$. Filled squares show the FIR excess observed from CS Cha and which cannot be attributed to a standard reprocessing accretion disk; open diamonds in optics show presumably the photospheric emission. [The lack, or negligibly low level, of emission in optical and NIR range from the accretion disk is considered as an indication of a hole in the inner disk (about 0.3 AU in size).]

For a rough estimate of the effects of mass loading on SEDs from accretion disks, one can use the following approximate expression for temperature in the region where heating due to dissipation of kinetic energy of falling clumps (first term in r.h.s. of eq. 18) reaches the maximum (at $x_m \sim \sqrt{L}$ with $(s/x)_m \sim e/L$)

$$\theta_m \sim \left[2(\gamma - 1) \frac{\Lambda - 1}{I} \frac{e}{L} \right]^{1/4}, \quad (25)$$

which correctly by order of magnitude describes the asymptotics at distances x where accretion heating (last two terms in eq. 18) and cooling due to mixing of cold infalling gas (second term in the l.h.s. in eq. 18) are unimportant – this region corresponds to the plateaus in $\theta(x)$ profiles in Figs. 2 and 3. In dimensional units $T_m \sim 0.8(\Lambda - 1)^{1/4} L^{-1/2} T_*$. For the above model it gives $T_m \sim 100$ K, and the corresponding frequency $\nu_m \sim 6 \times 10^{12}$ Hz.

2.4 Effects of angular momentum input

When infalling gas has non-zero angular momentum equation, so that $v_{c,\phi} \neq 0$ equation 3 is written in the form (Safronov & Vityazev 1983, Papaloizou & Lin 1995)

$$\frac{d}{dR}(\Sigma R^3 \Omega u_R) = \frac{d}{dR} \left(\nu \Sigma R^3 \frac{d}{dR} \Omega \right) + \Psi(R) R^2 v_{c,\phi}(R), \quad (26)$$

and the contribution to energy equation is determined by

$$\frac{2\pi}{M_0 R^2 \Omega} \int_{R_*}^R \Psi(R) R^2 v_{c,\phi}(R) dR. \quad (27)$$

In an extreme case when the angular velocity of the infalling gas approaches the keplerian value $v_{c,\phi}(R) = \sqrt{GM/R}$ energy equation reads as

$$\begin{aligned} \theta^4 + 6\delta \frac{\Lambda - 1}{I} \psi \theta &= 2(\gamma - 1) \frac{\Lambda - 1}{I} \frac{\psi}{x} + \frac{\Lambda}{x^3} \left(1 - \frac{1}{\sqrt{x}} \right) \\ &\quad - \frac{\Lambda - 1}{I} \frac{1}{x^3} \int_1^x \psi x dx + \frac{\Lambda - 1}{I} \frac{1}{x^{7/2}} \int_1^x \psi x^{3/2} dx. \end{aligned} \quad (28)$$

It is readily seen that for the mass input rate in the form eq. 20 the contribution from the last term is of the same order of magnitude (about 2/3) as of the third term, and thus never exceeds 30% for $\Lambda \sim 1$ and 3–6% for $\Lambda - 1 \ll 1$.

3 Conclusions

Dissipation of kinetic energy of clumpy gas falling onto accretion disks from the debris of a parent protostellar molecular cloud significantly alters the radial temperature distribution. It can be important in outer parts of a re-processing disk, where temperature decreases sufficiently $T \sim R^{-3}$, while the heat input rate associated with mass loading is approximately proportional to the square of the azimuthal velocity $\dot{E} \propto R^{-1}$. Thus, mass loading can naturally produce excess of emission in the long-wavelength range of SEDs of the accretion disks, and with an appropriate radial distribution of mass loading can reproduce observed FIR excess. For a one-peak radial distribution of the infall rate localized at $R \sim L$, the corresponding temperature in the hot ring for $R_* = 1 R_\odot$, $M_* = M_\odot$ is

$$T_m \sim 800 \left(\frac{\dot{M}_p}{\dot{M}_0} \right)^{1/4} \left(\frac{L}{1 \text{ AU}} \right)^{-1/2} \left(\frac{\dot{M}_0}{10^{-6} M_\odot \text{ yr}^{-1}} \right)^{1/4} \text{ K}, \quad (29)$$

and the wavelength

$$\lambda_m \sim 6 \left(\frac{L}{1 \text{ AU}} \right)^{1/2} \left(\frac{\dot{M}_p}{\dot{M}_0} \right)^{-1/4} \left(\frac{\dot{M}_0}{10^{-6} M_\odot \text{ yr}^{-1}} \right)^{-1/4} \mu\text{m}. \quad (30)$$

It is readily seen that the extra luminosity produced by the infalling gas is proportional to the mass loading rate, $L(\dot{M}_p) \sim \sigma T_m^4 L^2 \propto \dot{M}_p$, and for weak mass loading, $\dot{M}_p \ll \dot{M}_0$, is small as compared to the total luminosity of an unloaded disk. However, it can result in an observable effect if the loading mass is deposited at large radii, so that the wavelength in the peak of emission, eq. 30 falls into FIR range where the reprocessing disk does not contribute significantly. This case is shown in Fig. 6 where for mass loading $\dot{M}_p \sim 0.1\dot{M}_0$ the FIR luminosity of the infalling gas is approximately ten times smaller than the optical luminosity of the reprocessing disk.

The results presented in this paper have only an illustrative meaning, and can be directly applied for explanation of spectral features observed in protoplanetary disks only when clear evidences of mass loading will be found. Nonetheless, they definitely show that mass loading can have an important influence on temperature distribution in accretion disks and their spectra.

I thank S. A. Lamzin, A. V. Lapinov, A. M. Sobolev, I. I. Zinchenko for valuable discussions. This work was supported by RFBR (project No 99-02-16938) and INTAS (project No 1667). This research has made use of NASA's Astrophysics Data System Abstract Service.

References

- [1] Barnes, S., Tobin, W, Pollard, K. R. 2000, The variable CaII absorption in beta-Pictoris during 1998, Publ. Astron. Soc. Australia, 17, 241
- [2] Cowie, L. L., McKee, C. F., Ostriker, J. P. 1981, Supernova remnant revolution in an inhomogeneous medium. I - Numerical models, Astrophys. J., 247, 908

- [3] Falgarone, E., Phillips, T. G., Walker, C. K. 1991, The edges of molecular clouds - Fractal boundaries and density structure, *Astrophys. J.*, 378, 186
- [4] Grinin, V., Natta, A., Tambovtseva, L. 1996, Evaporation of star-grazing bodies in the vicinity of UX Ori-type stars, *Astron. & Astrophys.*, 313, 857
- [5] Hartquist, T. W., Dyson, J. E., Pettini, M., Smith, L. J. 1986, Mass-loaded astronomical flows. I - General principles and their application to RCW 58, *Month. Not. Roy. Astron. Soc.*, 221, 715
- [6] Klein, R. I., McKee, C. F., Colella, P. 1994, On the hydrodynamic interaction of shock waves with interstellar clouds. 1: Nonradiative shocks in small clouds, *Astrophys. J.*, 420, 213
- [7] Lecavelier des Etangs, A., Hobbs, L. M., Vidal-Madjar, A., Beust, H., Feldman, P. D., Ferlet, R., Lagrange, A.-M., Moos, W., & McGrath, M. 2000, Possible emission lines from the gaseous β Pictoris disk, *Astron. & Astrophys.*, 356, 691
- [8] Lynden-Bell, D., Pringle, J. E. 1974, The evolution of viscous discs and the origin of the nebular variables, *Month. Not. Roy. Astron. Soc.*, 168, 603
- [9] Natta, A., Meyer, M. R., & Beckwith, S. V. W. 1997, Circumstellar disks around pre-main-sequence stars: what ISO can tell us, In: *Star Formation with the Infrared space Observatory*, J. Zun & R. Liseau, eds, ASP Conference Series, v. 132, p. 265
- [10] Papaloizou, J. C. B., Lin, D. N. C. 1995, Theory Of Accretion Disks I: Angular Momentum Transport Processes, *Ann. Rev. Astron. Astrophys.*, 33, 505
- [11] Pringle, J. E. 1981, Accretion discs in astrophysics, *Ann. Rev. Astron. Astrophys.*, 19, 137
- [12] Roberge, A., Feldman, P. D., Lagrange, A. M., Vidal-Madjar, A., Ferlet, R., Jolly, A., Lemaire, J. L., Rostas, F. 2000, High-Resolution Hubble Space Telescope STIS Spectra of C I and CO in the β Pictoris Circumstellar Disk, *Astrophys. J.*, 538, 904

- [13] Safronov, V. S., Vityazev, A. V. 1983, The origin of Solar system, In: *Astrophysics and Cosmic Physics*, R. A. Sunyaev, ed., p. 5
- [14] Shakura, N. I., Sunyaev, R. A. 1973, Black holes in binary systems. Observational appearance, *Astron. Astrophys.*, 24, 337

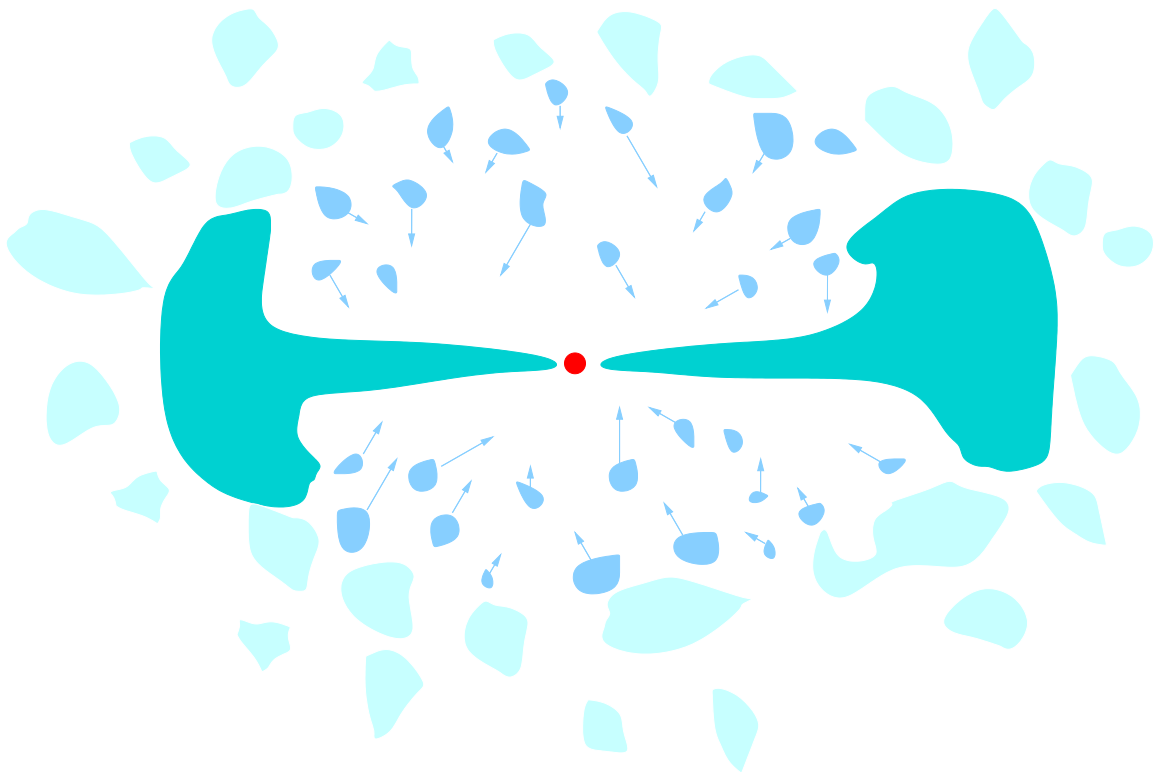


Figure 1: Schematic representation of the model: debris of the seed cloud falling down on the accretion protoplanetary disk.

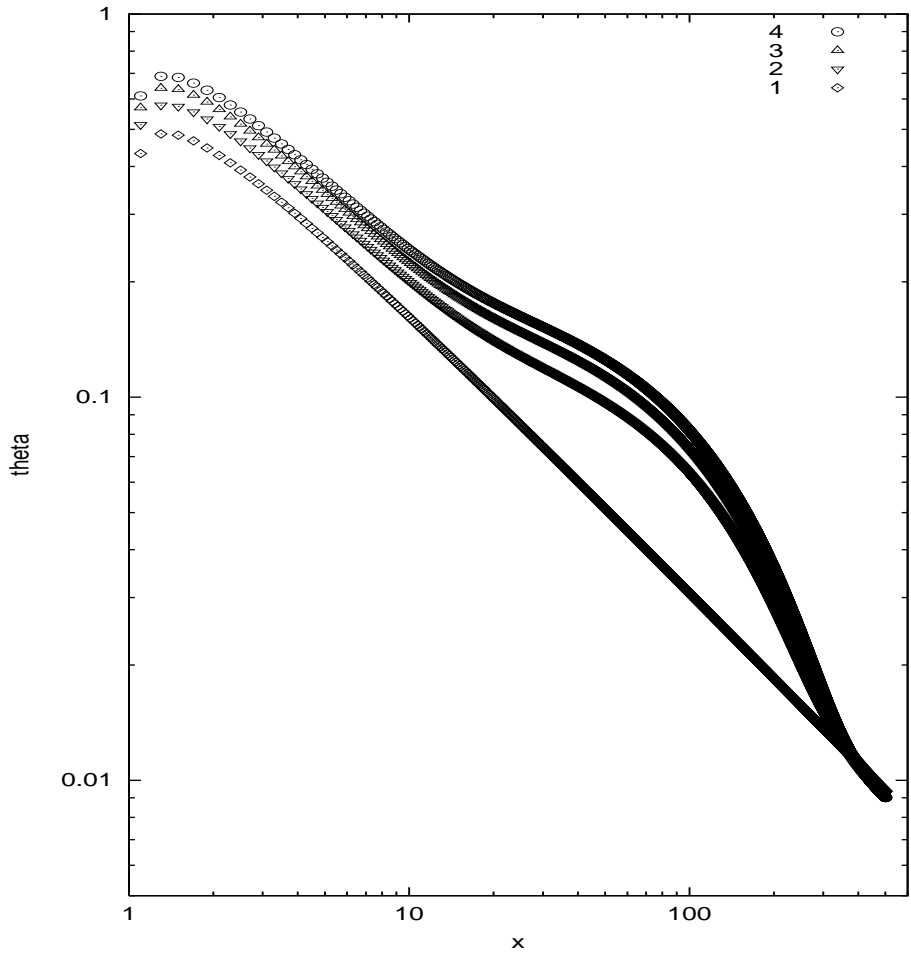


Figure 2: Temperature distribution $\theta(x)$ for the mass-loading function (20), $\delta = 10^{-3}$, $\Lambda = 1$ (unloaded), 2, 3, 4 from the bottom to top, $L = 30$.

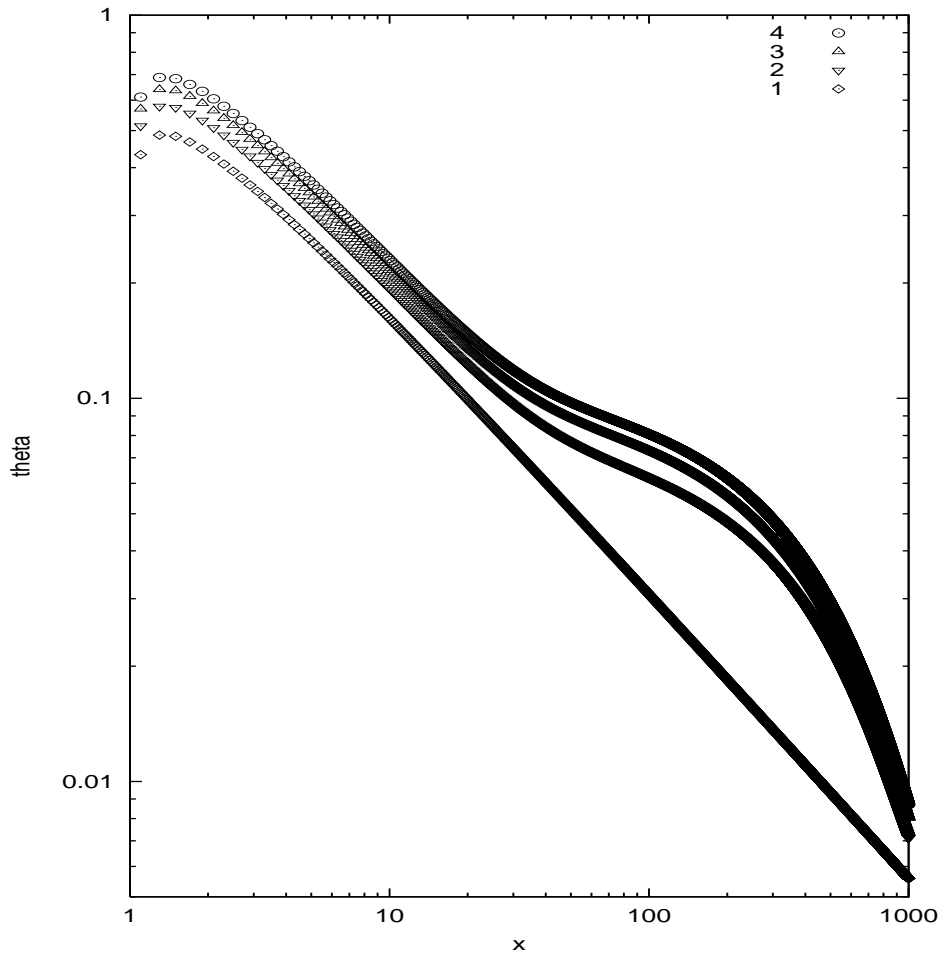


Figure 3: Same as in Fig. 2 for $L = 100$.

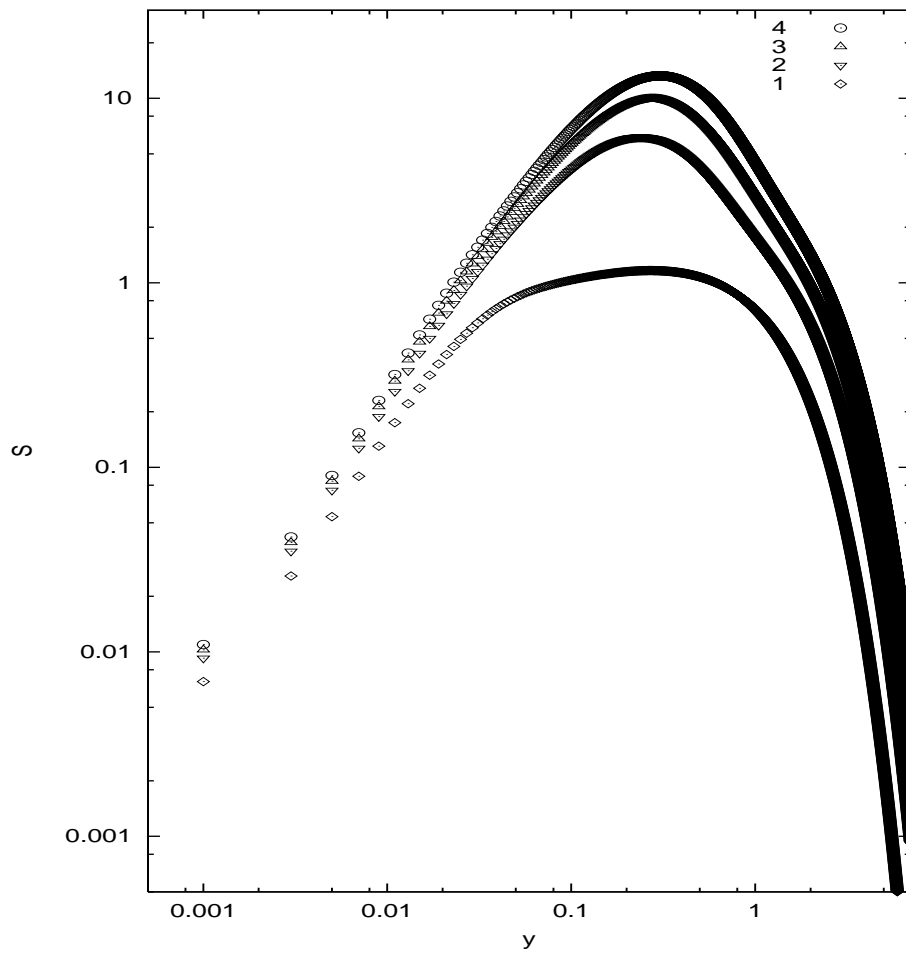


Figure 4: Energy spectrum for $\theta(x)$ shown in Fig. 2.

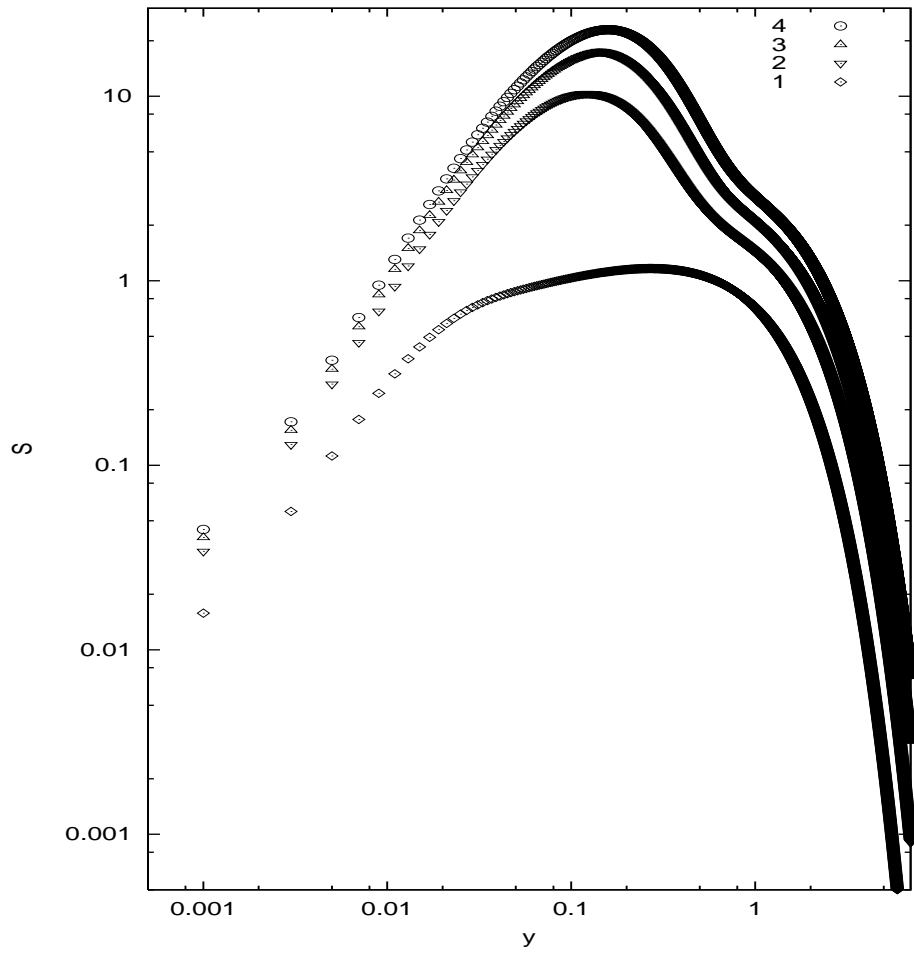


Figure 5: Same as in Fig. 4 for $L = 100$.

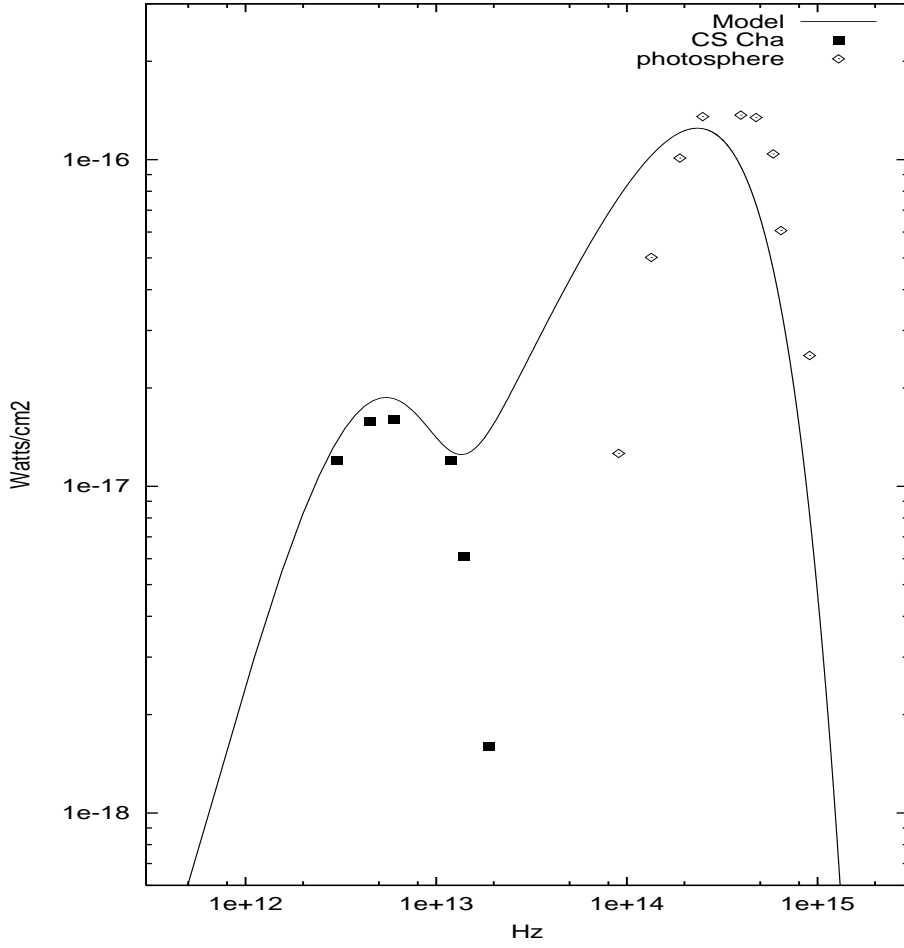


Figure 6: SED in CS Cha: open diamonds from ground-based observations (presumably represent the spectrum of the stellar photosphere), filled squares from ISO and IRAS – Natta, Meyer, & Beckwith (1997), solid line shows the spectrum of a mass-loaded disk with $\Lambda = 1.08$, $L = 9.2$ AU, $\dot{M}_0 = 2.2 \times 10^{-7} M_{\odot} \text{ yr}^{-1}$.